Available online at www.CivileJournal.org

Civil Engineering Journal

Vol. 5, No. 2, February, 2019

Displacement and Deformation of the First Tunnel Lining During the Second Tunnel Construction

Lin Wu [a*], Xiedong Zhang [a], Zhihua Zhang [a], Luqing Luo [a], Weichen Sun [b]

[a] *School of Transportation, Wuhan University of Technology, Peace Avenue,1178,Wuchang District, Wuhan, 430063, China.*

[b] *Hebei Chenya Technology Co. Ltd. Hebei, Shijiazhuang, 050056, China.*

Received 21 November 2018; Accepted 31 January 2019

Abstract

A three-dimensional twin tunnels scale model was established utilizing the discrete element method (DEM) with PFC3D. This model aims to investigate the displacement (in horizontal and vertical directions) and deformation of the first tunnel lining in four different cases which the clear distance of twin tunnels are 5, 10, 15 and 20 m during the second tunnel construction process. The numerical results indicate that the clear distance between twin tunnels and the distance between the measurement points of the first tunnel and the excavation area of the second tunnel are two most critical factors that influence the displacement and deformation of the first tunnel lining. Meanwhile, the soil arching effect, gravity, water pressure and lateral pressure also have an impact on the behavior of the first tunnel. The maximum disturbance of horizontal and vertical displacements occurred in the time points of finishing of the second tunnel. However, the horizontal displacement of the first tunnel is much more sensitive to the vertical displacement. The first tunnel turns to the right and down in direction while having an anticlockwise rotation (φ) during the process of construction of the second tunnel. In addition, the displacement and deformation of the lining of the first tunnel are critical to monitor, and the necessary precautions should be taken to decrease the risk of craze. In conclusion, the influence of the second tunnel excavation on the first tunnel lining could be neglected when their distance is more than 15 m.

Keywords: Twin-Tunnels; Tunnel Lining; Displacement; Deformation; Discrete Element Method (DEM).

1. Introduction

With the increase in transportation demand encountered in large cities, it is necessary to construct twin tunnels in the metro system. In the twin tunnels construction procedure, the second excavation of a tunnel (named Tunnel 2) will occur approximately one month after the first tunnel (named Tunnel 1) to reduce the disturbance to Tunnel 1 lining caused by the excavation of Tunnel 2. To avoid damage to the Tunnel 1 lining during and after the excavation for Tunnel 2, we should predict the influence caused by the Tunnel 2 construction on Tunnel 1 lining to choose the optimal clear distance for closely-spaced parallel shield twin tunnels.

Most of the previous study on twin tunnels are focused on the displacement of surface ground and tunnel surrounding soils [1-4], the analysis on the twin tunnels lining are relatively less. C.W.W. et al. [5] conducted several three-dimensional finite element models to investigate the multiple interactions between large parallel twin tunnels constructed by the new Austrian tunneling method. In this paper, the influence of lagging distance between the twin tunnels on the axial force and bending moment of tunnel lining have been highlighted. Do et al. [6-8] have simulated shield twin tunnels in soft ground using FLAC3D finite difference element programme. The influence of different distance in cross-section

* Corresponding author: wl256724@whut.edu.cn

http://dx.doi.org/10.28991/cej-2019-03091248

and longitudinal directions of twin tunnels on tunnels lining during tunnel excavation are discussed. Whereas, the distance between twin tunnels are relatively small (less than double of diameter). In this case, the construction influence between twin tunnels is obvious. Zhang et al. [9] have focused on the closed-form analytical solution for the prediction of liner internal forces induced by twin tunnels construction in clays using analysis method.

On the other hand, Particle Flow Code (PFC) is one type of Discrete Element Method (DEM) which is proposed by Cundall [10-11] has great advantages for modeling underground project such as tunnel in solid mechanics and granular flow. To date, previous DEM research on twin tunnels [12-14] has been limited to two-dimensional analysis using PFC2D, which does not capture the out-of-plane effects and realistically simulate the dynamic construction process of twin tunnels. As such, three-dimensional DEM modelling of twin tunnels is needed to assess the impact of adjacent tunnel constructional on an existing adjacent tunnel.

In view of these issues, there is still very limited knowledge of the displacement and deformation of an existing tunnel lining induced by later near distance tunneling, especially for the microscopic mechanism analysis by DEM method. To better understand the macro- and micro- mechanism of the lining of first tunnel during the construction process of the second tunnel using shield construction method, in this paper, a three-dimension DEM model has been conducted. In this model, the horizontal and vertical displacements and deformation of Tunnel 1 lining in four different cases have been discussed. The numerical results provide a reference for the distance of shield construction twin tunnels in cross section.

2. Model Setup

In the calculations process of DEM, Newton's second law is applied to the particles and the force-displacement law is used in the contacts between particles. The relationship between contact force and displacement is given in Equation (1-2). Newton's second law is used to determine the motion of each particle arising from the contact and body forces acting upon it, while the force-displacement law is used to update the contact forces arising from the relative motion at each contact. In the DEM simulation model, the interaction of particles is a dynamic process of equilibrium developing states. PFC3D can be treated as a simplified implementation of DEM because PFC3D simulates the assemblies of movement and interaction by rigid spherical particles, while the general DEM can adopt arbitrarily shaped particles.

$$F_i^n = K^n U^n n_i \quad (1)$$

$$\Delta F_i^s = -K^s \Delta U_i^s \quad (2)$$

Where F_i^n, K^n, U^n, and n_i are the normal contact force, the normal stiffness at the contact, the normal relative displacement and the normal unit vector, respectively. ΔF_i^s, K^s, and ΔU_i^s are the shear elastic force increment, the shear stiffness at the contact and the shear relative displacement, respectively.

A three-dimensional numerical model conducted by PFC is based on the Wuhan metro line 2 project. A scale model which the geometry size reduced the 20 times and the value of gravity remains unchanged are adopted in this paper. As a result, the corresponding parameters such as, modulus, displacement should be calculated based on similarity ratios [15-17]. The corresponding parameters are listed in the following figures and tables. The soil profile of the cross-river twin tunnels of the Wuhan metro and the selected cross section of analysis are presented in Figure 1. The schematic diagram of the Yangtze cross-river twin tunnels of the Wuhan metro and the corresponding measurement points of the first tunnel lining are shown in Figure 2a and 2b. The values in the figure are translated to the real project size. *L* is the clear distance of twin tunnels varies from 5 to 20 m. *D* and *d*, are outer and inner diameter of twin tunnels, their values are 6.52 m and 5.48 m, respectively. Tunnel lining which is made by C60 concrete and its thickness is 0.52 m. The basic parameters of each stratum and tunnel lining in the Yangtze cross-river twin tunnels of the Wuhan metro are shown in Table 1. After the process of particle parameter calibration, the micro-parameters of each surrounding stratum and C60 lining are shown in Table 2. The steps of the twin tunnels PFC3D model are as follows:

- **Step 1:** Creating a cubic structure composed of six walls with the size of 42×1.2×30 m (length× width × height) and generating small particles inside it. To improve computational efficiency, we simulate the following model using a larger particle size [18-19]. The radius of the particle in the surroundings is 0.007-0.012 m, and the radius of the particles in the lining are 0.003 m. The total number of particles is about 48000.
- **Step 2:** Consolidating the assembly with the calculated constant water pressure and lateral pressure ($P_W = P_L$=108 kPa) by the servo-system, and then applying the gravity and buoyancy for each particle.
- **Step 3:** Setting the micro-parameters of each stratum which is shown in Table 2, and then executing a certain cycle for reaching a quasi-static state.
- **Step 4:** Locating several measurement points in the model and excavating the Tunnel 1 by reducing the Tunnel 1 mechanical parameter of the particles in the excavation area to zero in limited cycles by ten steps. Installing the

concrete lining by setting a ring with the thickness of 0.52 m of C60. It is important to note that the excavation process can really simulate the tunneling process.

- **Step 5:** Cycling the model for a stable condition when there is no deformation of the surroundings around the Tunnel 1, and then excavating the Tunnel 2 with the same method in Step 4. The distribution of the measurement points in the Tunnel 1 lining is shown in Figure 2b.

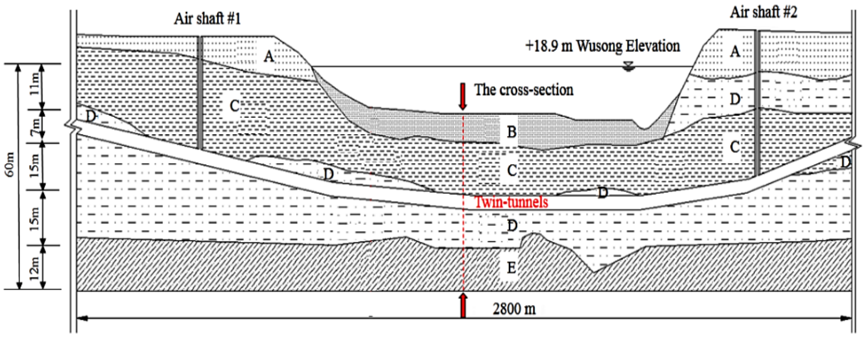

Figure 1. The soil profile of Yangtze cross-river twin tunnels of the Wuhan metro (B is silty clay, C is the coarse sand and contained with some gravel. D is the coarse sand and contained with some cobble.)

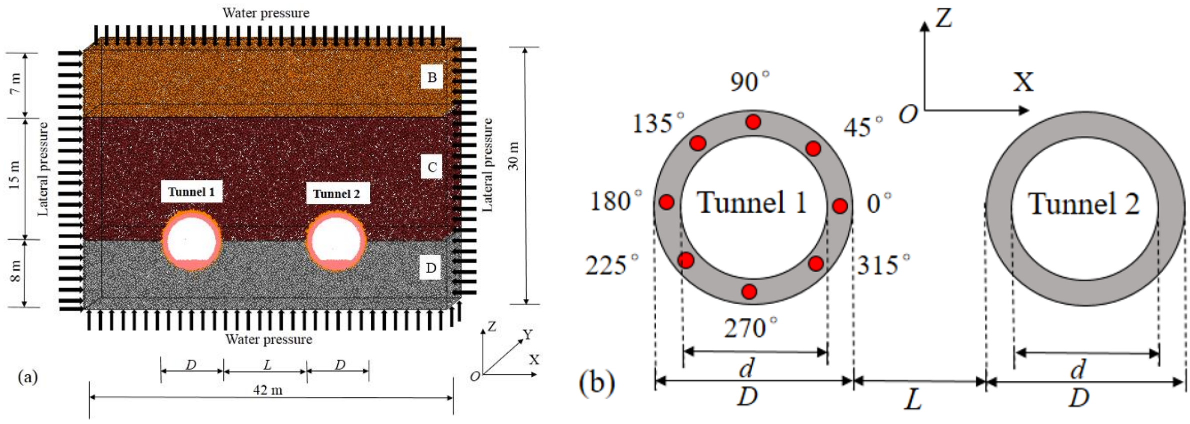

Figure 2. (a) Schematic diagram of the Yangtze cross-river twin tunnels of the Wuhan metro (b) The distribution of the measurement points in the first tunnel lining

Table 1. Basic parameters for each stratum and tunnel lining in the Yangtze cross-river twin tunnels of the Wuhan metro

Parameters	B	C	D	Lining
Density（kg/m^3）	1700	2050	2110	2180
Frictional angle（°）	10.5	42	40	70
Porosity	0.4	0.44	0.51	0.35
Modulus of compression（MPa）	2.17	35.4	38.1	36000
Moisture content (%)	49.5	16.1	18.0	—

Table 2. Micro-parameters of each surrounding stratum and C60 lining

Micro-parameters	B	C	D	Lining
Friction coefficient	0.185	0.9	0.84	1.98
Normal stiffness(N/m)	1.45×10^4	2.34×10^5	2.5×10^5	8.64×10^9
Shear stiffness (N/m)	5.8×10^3	9.36×10^4	1×10^5	3.456×10^9
Normal strength of contact bond (N)	67	0	0	—
Shear strength of contact bond (N)	67	0	0	—
Parallel bond radius multiplier	—	—	—	1.0
the Young’s modulus of each parallel bond (GPa)	—	—	—	36

Normal stiffness of parallel bond (N/m)	—	—	—	1.8×10^{11}
Shear stiffness of parallel bond (N/m)	—	—	—	7.2×10^{10}
Normal strength of parallel bond (Pa)	—	—	—	1×10^{8}
Shear strength of parallel bond (Pa)	—	—	—	1×10^{8}

3. Discussion and Results

For the purpose of exploring the mechanical behavior of the first tunnel lining during the excavation process of second tunnel, displacement and deformation of the first tunnel lining in four conditions of different twin tunnels clear distance such as L=5, 10, 15 and 20 m have been analyzed.

3.1. Horizontal Displacement

As shown in Figure 3, the variation process for horizontal displacement of Tunnel 1 lining can be divided into four stages. First stage: the horizontal displacements of Tunnel 1 lining increase with time domain when t is less than 0.085 s, which means the Tunnel 1 lining are gradually moving to the right direction. Second stage: the horizontal displacements of Tunnel 1 lining are reaching the peak values during 0.085 and 0.095 s. In these time points, the Tunnel 2 excavation is just finished. Third stage: when t = 0.095 - 0.135 s, the horizontal displacements generally decrease, which implies that the particles around Tunnel 1 are moving back to the left direction. Final stage: the measurement particles of Tunnel 1 lining nearly remain steady in the time of 0.135 - 0.177 s. Therefore, the whole measurement process is 0.177 s, and the final value of the horizontal displacements can be chosen at the time point of 0.177 s. In fact, the actual variation in the vertical displacements of Tunnel 1 lining are similar to the rule of the horizontal displacements.

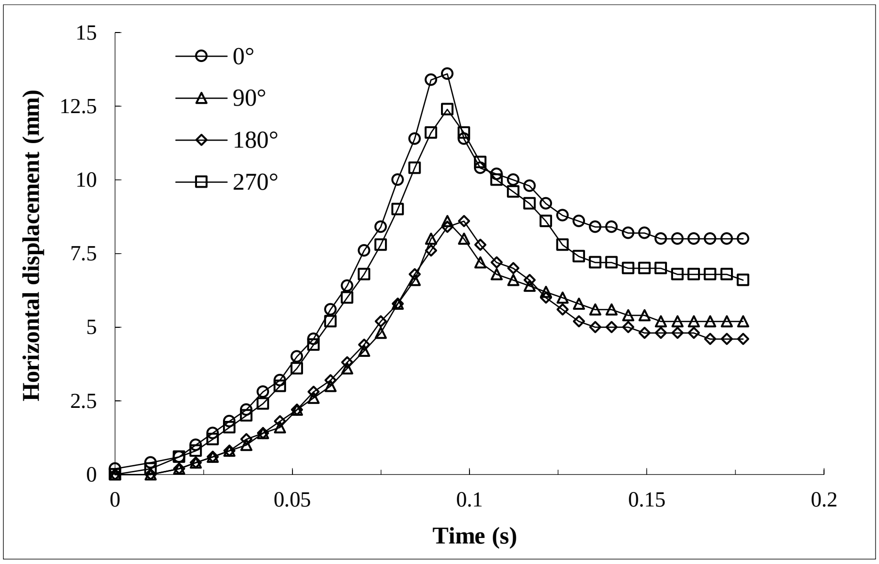

Figure 3. The horizontal displacement of Tunnel 1 lining during Tunnel 2 excavation in case of *L*=5 m

The peak and final horizontal displacements of Tunnel 1 lining can reflect the maximum and residual horizontal disturbance of Tunnel 1 caused by Tunnel 2 tunneling. Consequently, the peak and final horizontal displacements of Tunnel 1 were analyzed, and their values at the different measurement points are shown in Figure 4a and 4b.

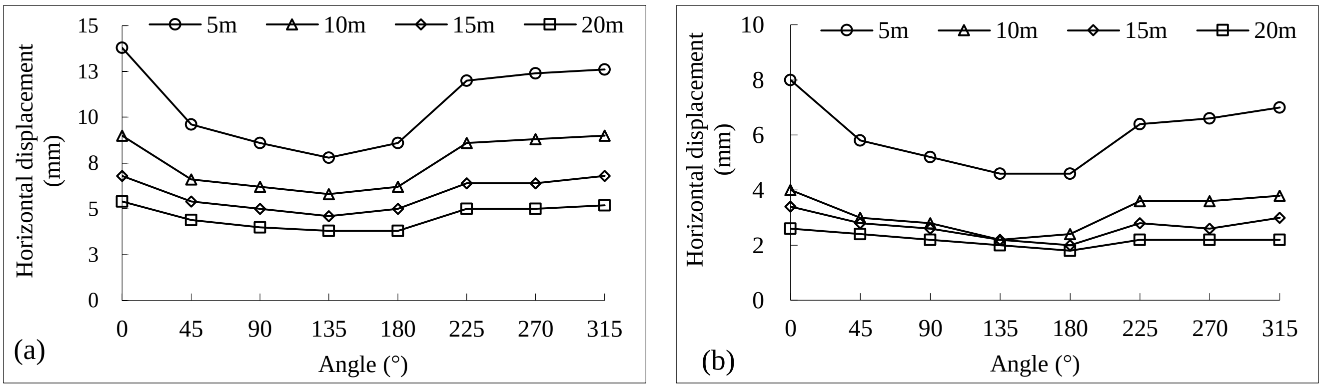

Figure 4. (a) Peak horizontal displacement, (b) Final horizontal displacement of Tunnel 1 during Tunnel 2 excavation at different measurement points

During Tunnel 2 excavation, the peak and final horizontal displacements of Tunnel 1 lining are positive, reflecting the Tunnel 1 lining generally towards the Tunnel 2 direction. In the simulation process, the stiffness and cohesive bond of the particles in the excavation area of Tunnel 2 are reduced to zero in limited cycles by ten steps. This practice will produce an unloading effect [20]. Meanwhile, under the action of lateral earth pressure, the Tunnel 1 lining has a trend to move to the Tunnel 2 position.

When the clear distance of twin tunnels (*L*) varies from 5 to 20 m, the peak and final horizontal displacements of Tunnel 1 lining decrease. If *L* is larger than 15 m, the peak and final horizontal displacements change only slightly. Meanwhile, the peak and final horizontal displacements in the left semicircle of the Tunnel 1 lining (e.g., 0°, 45°, 315°) are larger than the values of the right semicircle (e.g., 135°, 180°, 225°). These phenomena explain that the clear distance of twin tunnels and the distance of measurement points and excavation area are significant factors that influence the peak and final horizontal displacements, whereas the impact on Tunnel 1 lining can be ignored when *L* is larger than 15 m.

It is remarkable that, for horizontal displacements of Tunnel 1 lining, the peak values are approximately twice the final values. The Tunnel 1 lining reaches the peak horizontal displacement and the Tunnel 2 is exactly constructed, simultaneously. Then, the formation of the arching effect [13, 21] and the installed lining of Tunnel 2 create an intense restriction to prevent the trend of right towards the movement of Tunnel 1 lining. Furthermore, the greater stability and larger stiffness of Tunnel 2 make Tunnel 1 lining move back by the rebound effect.

3.2. Vertical Displacement

The peak and final vertical displacements of Tunnel 1 lining have similar rule with corresponding horizontal displacements, which are shown in Figure 5a and 5b. The difference rules are as follows:

During Tunnel 2 excavation, the value of the peak vertical displacements of Tunnel 1 are negative, which means that the Tunnel 1 lining is turning down. Under the combined action of water pressure and gravity, the particles around Tunnel 1 move down. The peak and final vertical displacements of Tunnel 1 lining are almost the same (see Figure 5a and 5b), while the final horizontal displacement are much smaller than the peak horizontal displacement (see Figure 4a and 4b), which means the period after Tunnel 2 excavation time have little influence on vertical displacement of Tunnel 1 lining whereas have great influence on horizontal displacement.

The vertical displacements are relatively small, implying that the sense of horizontal displacement of Tunnel 1 is stronger than the sense of vertical displacement for the parallel shield twin tunnels. In contrast to the horizontal and vertical displacements at θ=0° (see Figure 4 and Figure 5), the outstanding difference in the horizontal and vertical displacements can be attributed to the translated way of the Tunnel 2 tunneling disturbance as a horizontal wave. As a result, the peak and final horizontal displacements are larger at the horizontal points (e.g., θ=0°).

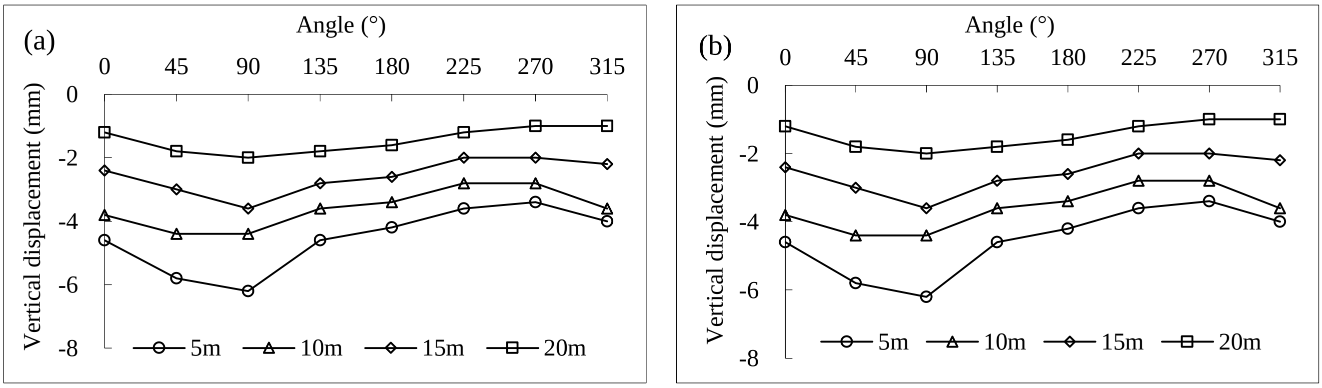

Figure 5. (a) Peak vertical displacement; (b) Final vertical displacement of Tunnel 1 during Tunnel 2 excavation at different measurement points

3.3. Deformation of Lining

Combined the horizontal and vertical displacements of Tunnel 1 lining, the displacement and deformation of the Tunnel 1 lining for the different values of *L* (5 m, 10 m, 15 m and 20 m) are shown in Figure. 6, where the displacement is the vector sum of the horizontal and vertical displacements. R_0 is the average value of the outer and inner radius of Tunnel 1 lining.

The displacement of the Tunnel 1 lining is clearly observed in the graphs. The lining of Tunnel 1 turns to the right and down in direction, meanwhile having an anticlockwise rotation (φ) during the process of Tunnel 2 construction. As the distance of twin tunnels increased (*L*), the anticlockwise rotation (φ) decreased. This can be explained by the construction effect of Tunnel 2 on the anticlockwise rotation of Tunnel 1 become smaller as the distance of twin tunnels increasing.

Considering the deformation of the Tunnel 1 lining, the vault and bottom of the lining are compressed, while the horizontal points (e.g., 0° and 180°) are stretched during the process of Tunnel 2 construction. The deformation of the Tunnel 1 lining in the right semicircle are larger than the deformation of the Tunnel 1 lining in the left semicircle. The results are in good agreement with the results of Mohammad *et al.* [22], where the clearance distance of the twin tunnels is 8 m and the diameter of the tunnels is 6 m in the paper.

In the process of the construction of Tunnel 2, the enormous effect on the Tunnel 1 lining raises the risk of crack. Some effective practices are adopted to reinforce the concrete of the tunnel lining. High performance concrete of C60 is used in this model. Buratti *et al.* [23] and Meng *et al.* [24] investigate the advantages of using Steel Fiber Reinforced Concrete (SFRC) for the tunnel lining. The SFRC tunnel lining can significantly reduce the crack width opening for a given stress field and satisfy the design criteria for load carrying ability and crack width. The combination of steel fiber and concrete indicates an optimal choice of reinforcement for a tunnel lining.

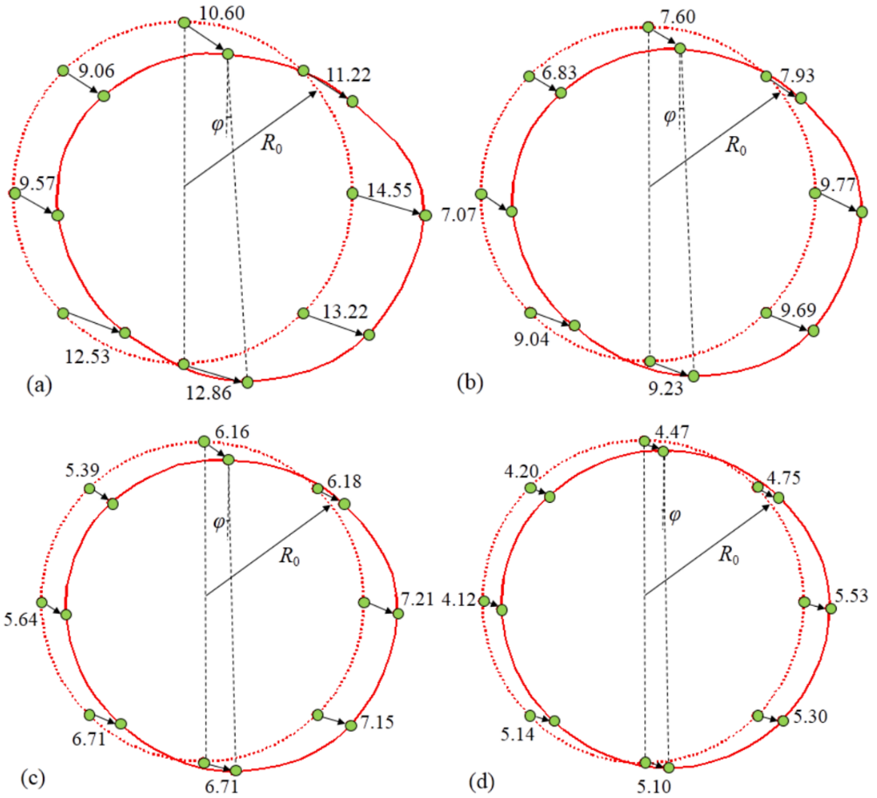

Figure 6. The displacement and deformation of Tunnel 1 lining during Tunnel 2 excavation when *L* are (a) 5 m; (b) 10 m; (c) 15 m; (d) 20 m (R_0=3.0 m, displacement :mm)

4. Conclusions

- The variation process for the horizontal displacement of Tunnel 1 lining can be divided into four stages, similar to the rule of vertical displacement. The maximum disturbance occurs at the time points when Tunnel 2 is finished. As the twin tunnel distance increases, horizontal and vertical displacements accordingly decrease. The horizontal displacement of the Tunnel 1 is much more sensitive to the Tunnel 2 construction than the vertical displacement. These different horizontal and vertical displacements at the measurement points of Tunnel 1 lining explain the uneven deformation and various displacements. These phenomena will produce unsteadiness for the twin tunnels.
- Tunnel 1 lining turns to the right and the downward direction and has an anticlockwise rotation (φ) during the process of Tunnel 2 construction. The vault and bottom of the lining are compressed, while the horizontal points are stretched during the process of Tunnel 2 construction. The deformation of the Tunnel 1 lining in the right semicircle are larger than the deformation of the Tunnel 1 lining in the left semicircle. High performance concrete and SFRC concrete lining can effectively reduce the crack width and reinforce the tunnel lining.
- The clear distance of twin tunnels (L) and the distance of the measurement points to the second tunnel excavation area are the two significant factors to affect the mechanical behavior such as the displacement and deformation of the first tunnel. The influence of the Tunnel 2 excavation on Tunnel 1 could be neglected when their distance is more than 15 m.

5. Funding

The authors thank the financial supports from the National Natural Science Foundation of China (No. 51408450).

6. Conflict of Interest

The authors declare no conflict of interest.

7. References

[1] Chapman, D.N., Ahn, S.K., and Hunt, D.V.L. "Investigating Ground Movements Caused by the Construction of Multiple Tunnels in Soft Ground Using Laboratory Model Tests." Canadian Geotechnical Journal, 44, no. 6 (January 22, 2007): 631–643, doi:10.1139/t07-018.

[2] Chu, Bin-Lin, Hsu, Sung-Chi, Chang, Yi-Long, and Lin, Yeong-Shyang. "Mechanical behavior of a twin-tunnel in multi-layered formations." Tunnelling and Underground Space Technology 22 (June 15, 2006): 351-362, doi: 10.1016//j.tust.2006.06.003.

[3] Choi, Jung-In. and Lee, Seok-Won. "Influence of Existing Tunnel on Mechanical Behavior of New Tunnel." KSCE Journal of Civil Engineering, 14, no. 5 (December 24 2009): 773-783, doi: 10.1007/s12205-010-1013-8.

[4] Li, Peng, Du, Shou-Ji, Ma, Xian-Feng, Yin, Zhen-Yu, and Shen, Shui-Long. "Centrifuge Investigation into the Effect of New Shield Tunnelling on an Existing Underlying Large-diameter Tunnel." Tunnelling and Underground Space Technology 42 (February 2, 2014): 59-66, doi: 10.1016/j.tust.2014.02.004.

[5] C.W.W. Ng, K.M. Lee, and D.K.W. Tang. "Three-dimensional Numerical Investigations of New Austrian Tunnelling Method (NATM) Twin Tunnel Interactions." Canadian Geotechnical Journal 41(June 30, 2004): 523-539, doi: 10.1139/t04-008.

[6] Do, Ngoc-Anh, Dias, Daniel, Oreste, Pierpaolo, and Djeran-Maigre, Irini. "Three-dimensional Numerical Simulation of a Mechanized Twin Tunnels in Soft Ground." Tunnelling and Underground Space Technology 42 (February 25, 2014): 40-51, doi:10.1016//j.tust.2014.02.001.

[7] Do, Ngoc-Anh, Dias, Daniel, and Oreste, Pierpaolo. "3D Numerical Investigation on the Interaction between Mechanized Twin Tunnels in Soft Ground." Environmental Earth Sciences, 73, no. 5 (August 1, 2014): 2101-2113, doi: 10.1007/s12665-014-3561-6.

[8] Do, Ngoc-Anh, Dias, Daniel, and Oreste, Pierpaolo. "3D Numerical Investigation of Mechanized Twin Tunnels in Soft Ground – Influence of Lagging Distance Between Two Tunnel Faces." Engineering Structures 109 (December 17, 2015): 117-125, doi:10.1016/j.engstruct.2015.11.053.

[9] Zhang, Zhiguo, Zhang, Mengxi, Jiang, Yunjuan, Bai, Qiaomu, and Zhao, Qihua. "Analytical Prediction for Ground Movements and Liner Internal Forces Induced by Shallow Tunnels Considering Non-uniform Convergence Pattern and Ground-liner Interaction Mechanism." Soil and Foundations 57 (April 13, 2017): 211-226, doi: 10.1016/j.sandf.2017.03.004.

[10] Cundall, P.A. "A Computer Model for Simulating Progressive Large Scale Movements in Blocky Rock Systems." Proceedings of International Symposium on Rock Mechanics, Rock Fracture, 1971, Nancy, France: 2-8.

[11] Cundall, P.A. and Strack, O.D.L. "A Discrete Numerical Model for Granular Assemblies." Géotechnique, 29, no. 1, 1979: 47-75, doi: 10.1680/geot.1979.29.1.47.

[12] Funatsu, T., Hoshino, T., Sawae, H., and Shimizu, N. "Numerical Analysis to Better Understand the Mechanism of Effects of Ground Supports and Reinforcements on the Stability of Tunnels Using the Distinct Element Method." Tunnelling and Underground Space Technology 23 (December 3, 2007): 561-573, doi: 10.1016/j.tust.2007.10.003.

[13] He, Chuan, Feng, Kun, Fang, Yong, and Jiang, Ying-chao. "Surface Settlement Caused by Twin-parallel Shield Tunnelling in Sandy Cobble Strata." Journal of Zhejiang University-SCIENCE A, 13, no. 11, (September 27, 2012): 858-869, doi:10.1631/jzus.A12ISGT6.

[14] Oliaei, M. and Manafi, E. "Static Analysis of Interaction Between Twin-tunnels Using Discrete Element Method (DEM)." Scientia Iranica, 22, no. 6, (May 30, 2015):1964-1971.

[15] Rocha, M. "The Possibility of Solving Soil Mechanics Problems by Use of Models." Proceedings of 4th International Conference Soil Mechanism. Fdn. England. London, 1 (1957): 83-88.

[16] Fang, Yong, Xu, Chen, Cui, Ge, and Kenneally, Bernadette. "Scale Model Test of Highway Tunnel Construction Underlying Mined-out Thin Coal Seam." Tunnelling and Underground Space Technology 56 (March 24, 2016):105–16, doi:10.1016/j.tust.2016.03.007.

[17] Wu, Lin, Zhang, XieDong, Zhang, ZhiHua, and Lin, FaJin. "The Vertical and Horizontal Displacement of Cross-river Twin-tunnels Surroundings Induced by Tunneling." International Association for Bridge and Structural Engineering (IABSE) Conference, Kuala Lumpur 2018: Engineering the Developing World-Report: 838-844.

[18] Gu, Xiaoqiang, Lu, Lutong, and Qian Jiangu. "Discrete Element Modeling of the Effect of Particle Size Distribution on the Small Strain Stiffness of Granular Soils." China Particuology 32 (2017):21-29, doi: 10.1016/j.partic.2016.08.002.

[19] Lu, J.F, Zhang, C.W., and Jian, P. "Meso-structure Parameters of Discrete Element Method of Sand Pebble Surrounding Rock Particles in Different Dense Degrees." Proceedings of the 7th international Conference on Discrete Element Methods, (Cat. No.20165303205315) 2017; 188: 871-879.

[20] Jiang, Mingjing, and Yin, Zhen-Yu. "Analysis of Stress Redistribution in Soils and Earth Pressure on Tunnel Lining Using the Discrete Element Method." Tunnelling and Underground Space Technology, 32, no. 6, (June 28, 2012): 251-59, doi:10.1016/j.tust.2012.06.001.

[21] Rui, Rui, Tol, Frits van, Xia, Xiao-Long, Eekelen, Suzanne van, Hu, Gang, and Xia Yuan-you. "Evolution of Soils Arching; 2D DEM Simulations." Computers and Geotechnics 73 (December 29, 2015): 199-209.

[22] Afifipour, Mohammad, Sharifzadeh, Mostafa, Shahriar, Kourosh, and Jamshidi, Hamed. "Interaction of Twin Tunnels and Shallow Foundation at Zand Underpass, Shiraz metro, Iran." Tunnelling and Underground Space Technology, 26, no. 2, (December 3, 2010): 356-363, doi: 10.1016/j.tust.2010.11.006.

[23] Buratti N., Ferracuti B., and Savois M. "Concrete Crack Reduction in Tunnel Linings by Steel Fibre-reinforced Concretes." Construction and Building Materials 44 (April 9, 2013): 249-259, doi: 10.1016/j.conbuildmat.2013.02.063.

[24] Meng GW, Gao B, Zhou JM, Cao GD, and Zhang Q. "Experimental Investigation of the Mechanical Behavior of the Steel Fiber Reinforced Concrete Tunnel Segment." Construction and Building Materials 126 (September 12, 2016): 98-107, doi:10.1016/j.conbuildmat.2016.09.028.